Fluid Dynamics & Materials Processing FDMP, vol.15, no.4, pp.403-417, 2019

Experimental and Theoretical Analysis of the Drag Torque in Wet Clutches

Haojie Pan[1, *] and Xiaojun Zhou[1]

Abstract: Traditional mathematical models cannot predict and explain the phenomenon by which the drag torque (DT) in wet clutches rises in the high-speed zone. In order to evaluate the DT in such conditions, a two-phase air-fluid mathematical model for a DT with grooves was elaborated. The mathematical model was based on the theory of viscous fluid flow. A two-phase volume of fluid model was also used to investigate the distribution and volume fraction of air and fluid. Experiments on three friction plates with different grooves were conducted to validate the resulting mathematical model. It was found that the gap between plates decreased in the high-speed zone, thereby producing an increase of the DT in the high-speed zone. These results support the understanding of the physical phenomena relating to disengaged wet clutches, and provide a theoretical basis for the future improvement of drive systems.

Keywords: Wet clutch, drag torque, two-phase fluid, groove form.

1 Introduction

The wet multiplate friction clutch is a key component of the powertrain system. Owing to its compact structure, high power density, and smooth shifting, it is widely used in the transmission system of vehicles and ships, especially heavy vehicles and large construction vehicles. As shown in Fig. 1, the wet clutch generally consists of friction plates, separator plates, and a piston pressure plate. The lubricating fluid flows into the friction pair through the fluid inlet hole of the inner hub, and flows out through the fluid outlet of the outer hub. When the clutch is disengaged, the relative movement of the friction plate and separator plate will cause viscous shearing of the fluid film in the gap between the disks. This results in a drag torque (DT) on both the disks and causes power loss, which is the main factor affecting fuel economy. Therefore, the DT of the wet clutch has been widely researched all over the world.

In the 1970s, Lloyd et al. concluded that the most important factor affecting the DT was the relative rotational speed of the friction plate and separator plate [Lloyd (1974)]. The simplest quantitative study of the DT of wet clutches was based on the assumption of full fluid film and laminar flow. Kitabayashi first deduced the theoretical model of the DT, which was based on Newton's internal friction law [Kitabayashi and Hiraki (2003)]. This

[1] School of Mechanical Engineering, Zhejiang University, Hangzhou, 310000, China.

[*] Corresponding Author: Haojie Pan. Email: pan_haojie@zju.edu.cn.

model described the change in torque in the low-speed stage, but was unable to explain why the torque decreased at medium and high speed.

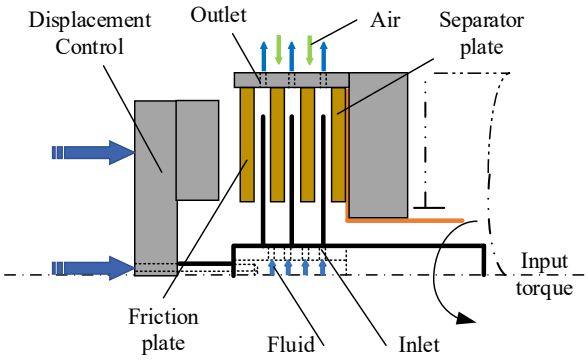

Figure 1: Wet multiplate clutch model

Kato established a DT model by considering the centrifugal force, which revealed that film shrinkage caused by centrifugal force was the reason for the reduction in DT [Kato (1993)]. This laid the foundation for the study of the mathematical DT model. Based on the Kato's model, Yuan et al. proposed the concept of fluid film equivalent radius and provided the shape of the fractured fluid film [Yuan and Hill (2007)]. Alphale et al. used the groove ratio to estimate the DT with the grooved friction plate [Aphale, Cho, Schultz et al. (2006)]. Later, Yuan et al. [Yuan, Peng and Jing (2011)] proposed the existence of a two-phase gas-liquid region in the fluid film rupture zone, and estimated the DT according to the continuous fluid film area [Yuan, Guo Hu et al. (2010)]. Shoaib Iqbal et al. [Iqbal, Albender, Pluymers et al. (2013)] considered the full fluid lubrication area, two-phase gas-liquid coexistence area, and fluid mist area on the basis of Yuan et al. They investigated the high speed range of 4500-5000 rpm, and found that the torque rose again in the high speed range [Iqbal, Albender, Pluymers et al. (2014)]. Pahlovy et al. [Mahmud, Pahlovy, Kubota et al. (2017); Pahlovy, Mahmud, Kubota et al. (2017)] also investigated the torque in the high speed range of 6000-10000 rpm, and found that decreased clearance increased the DT.

In summary, although researchers have done quite a lot of work to improve the DT model, the model still needs improvement. At present, most models do not consider the groove form and parameters, and friction plate material. Moreover, the reason why the DT rises again remains unknown, and research on DT in real working conditions is lacking.

In this paper, experimental and numerical simulations were used to study the DT in wet clutches, and a mathematical model for predicting the DT of disengaged wet clutches in the high-speed region with groove consideration was proposed.

2 Mathematical model

A friction pair of wet clutches was taken as the research object, as shown in Fig. 2.

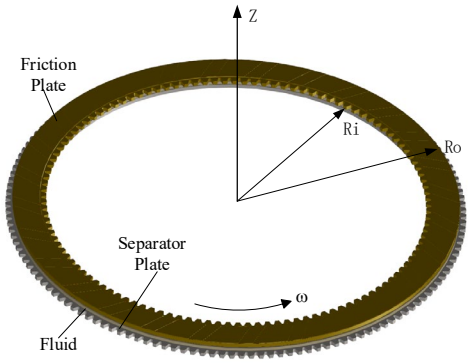

Figure 2: Drag torque simplified analysis model

We used the Navier-Stokes equation to solve the problem. The simplified Navier-Stokes equation can be expressed as Hu et al. [Hu, Peng and Wei (2012)]

$$\begin{cases} \rho\left(v_r\dfrac{\partial v_r}{\partial r}-\dfrac{v_\theta^2}{r}\right)=-\dfrac{\partial p}{\partial r}+\mu\dfrac{\partial^2 v_r}{\partial z^2} \\ \rho\left(v_r\dfrac{\partial v_\theta}{\partial r}+\dfrac{v_r v_\theta}{r}\right)=\mu\dfrac{\partial^2 v_\theta}{\partial z^2} \\ \dfrac{\partial p}{\partial z}=0 \end{cases}, \tag{1}$$

where v_r is the radial velocity; v_θ is the circumferential velocity; ρ is the lubricating fluid density; μ is the lubricating fluid dynamic viscosity; and p is the pressure distribution; r, θ, and z are the three directions of the cylindrical coordinate system.

According to the nonslip wall condition [Xiang, Zhang and Liu (2013)], the boundary condition of (1) is

$$\begin{cases} v_r(r,0)=0, v_r(r,h)=0 \\ v_\theta(r,0)=0, v_\theta(r,h)=\omega r, \\ P_o=0, P_i=0 \end{cases} \tag{2}$$

where P_o, P_i are the pressure at the inlet and outlet of the lubricating fluid, h is the gap thickness. and ω is the relative angular velocity.

The approximate solution of (1) using iteration method and substituting the boundary condition (2) is

$$v_r=\frac{1}{2\eta}\frac{dp}{dr}(z^2-zh)+\frac{\rho r\omega^2}{12\eta h^2}(zh^3-z^4) \tag{3}$$

2.1 Full oil film lubrication flow model

Assuming that the gap is full of flow, we can obtain the model of flow rate by

considering friction plates with three typical groove forms.

(1) Nongroove friction plate

The flow rate Q_1 through the gap between the disks without grooves can be obtained as

$$Q_1=2\pi r\int_0^h v_r dz=-\frac{\pi h^3 r}{6\mu}\frac{dp}{dr}+\frac{\pi\rho\omega^2 r^2 h^3}{20\mu} \tag{4}$$

(2) Radial groove friction plate

The flow rate Q_2 through the gap between the disks with radial grooves can be obtained as

$$\begin{aligned} Q_2&=2\pi rk\int_0^{h_1} v_r dz+2\pi r(1-k)\int_0^h v_r dz \\ &=-\frac{\pi h_1^3 rk}{6\mu}\frac{dp}{dr}+\frac{\pi\rho\omega^2 r^2 h_1^3 k}{20\mu}+(1-k)(-\frac{\pi h^3 rk}{6\mu}\frac{dp}{dr}+\frac{\pi\rho\omega^2 r^2 h^3 k}{20\mu}) \end{aligned} \tag{5}$$

where k is the ratio of the groove arc to the total arc; and h_1 is the thickness of the groove.

(3) Double arc groove friction plate

According to the structure of the double arc groove friction plate, the flow rate is between that of the nongroove friction plate and radial groove friction plate [Li, Khonsari, Mccarthy et al. (2014)]. Thus, we introduce a flow correction coefficient c to indicate the flow rate of the double arc groove friction plate Q_3 as

$$Q_3=(1-c)Q_1+cQ_2 \tag{6}$$

2.2 Film shrinkage model

The result of the full oil film lubrication flow model is shown in Fig. 3. It can be seen that as the rotational speed increases, the flow rate required to maintain full oil film lubrication also increases.

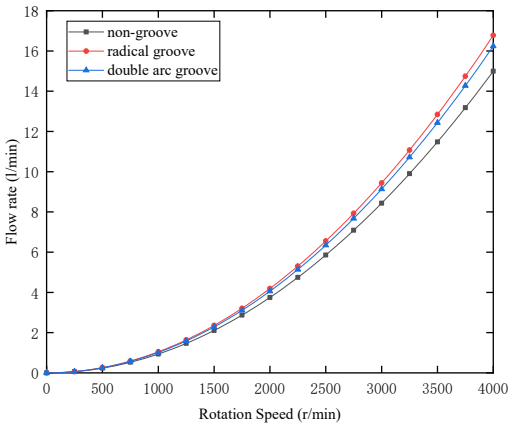

Figure 3: Flow rate required for full film lubrication of three grooves

Table 1: Parameters for simulation

Parameters	ρ (kg/m^3)	*Ri* (mm)	*Ro* (mm)	*h* (mm)	μ (Pa.s)	ω (rpm)	*c*	Q_a *(l/min)*
Values	870	188	214	0.5	0.068	4000	0.7	0.5

However, the given flow rate is generally a constant value. If the actual lubricant flow rate between the friction pairs is less than the required lubricant flow rate, then the oil film between the friction pairs will shrink [Takagi, Okano, Miyayaga et al. (2012)], as shown in Fig. 4.

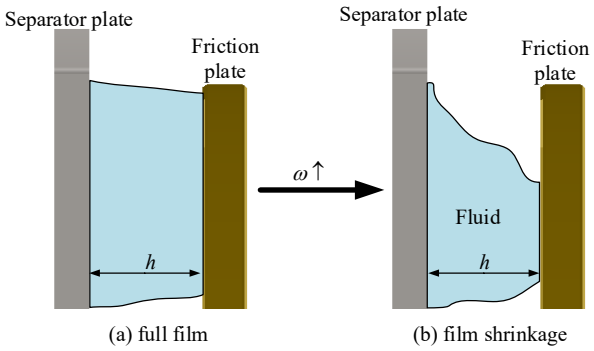

Figure 4: Oil film shrinkage schematic

According to Reynolds cavity boundary conditions:

$dp/dr = 0$.

$$\frac{\pi\rho\omega^2 h^3}{20\mu}r^4 - r^2 Q + \frac{9\rho Q^2 h}{140\pi\mu} = 0. \tag{7}$$

The radius expression of the full fluid film coverage area is obtained by (6):

$$r^* = \begin{cases} R_o, Q_a > Q \\ \sqrt{\dfrac{10\mu Q - 10\mu\sqrt{\dfrac{Q^2 - 9\rho^2 Q^2 \omega^2 h^4}{700\mu^2}}}{\pi\rho\omega^2 h^3}}, Q_a \le Q \end{cases}, \tag{8}$$

where R_o is the outer diameter, Q_a is the supplied flow rate, and h is the fluid film thickness.

Meanwhile, the expression of the fluid phase volume fraction φ can be obtained by using the Reynolds boundary condition:

$$Q_a = \varphi 2\pi r \int_0^h v_r dz$$
$$\varphi = \frac{20\mu Q_a}{\rho\pi r^2 h^3 \omega^2}. \tag{9}$$

From the above, it can be seen that as the relative rotational speed of the friction pair increases, the given flow rate cannot maintain full oil film lubrication, and the oil film shrinks. The gap is in two-phase flow state.

2.3 Gap shrinkage model

According to the traditional model, as the speed further increases, the DT will continuously decrease. However, in practical applications, it was found that as the speed continues to increase, the DT also increases. Therefore, further analysis of the DT at higher speed is required.

Integrating Eq. (3) results in the pressure radial distribution expression:

$$p(r) = -\frac{6\mu Q}{\pi h^3}\ln\frac{r}{R_o} + \frac{3\rho\omega^2}{20}(r^2 - R_o{}^2). \tag{10}$$

The pressure of the lubricant is integrated over the entire friction surface to obtain the lubricant film support force F_f:

$$F_f = 2\pi \int_{R_i}^{R_s} p(r) r dr. \tag{11}$$

Substituting Eq. (10) into Eq. (11):

$$F_f = \frac{6\mu Q}{h^3}\left(-R_s^2 \ln\frac{R_s}{R_o} - R_i^2 \ln\frac{R_o}{R_i} + \frac{R_s^2 - R_i^2}{2}\right) + \frac{3\pi\rho\omega^2(R_s^4 - 2R_s^2R_o^2 - R_i^4 + 2R_i^2R_o^2)}{40} \tag{12}$$

As shown in Fig. 5, the fluid film supporting force has a negative value under certain conditions with the increase in rotational speed.

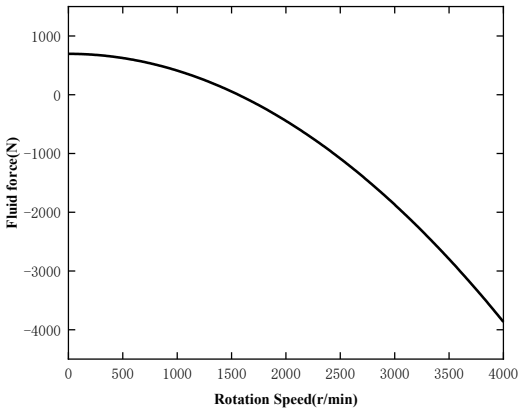

Figure 5: Fluid force

Applying force analysis to the separator plate yields the following expression:

$$F_f + F_{fa} - F_a = 0, \tag{13}$$

where F_f is the film support force, F_{fa} is the force of air in the gap, and F_a is the force of air out of the gap.

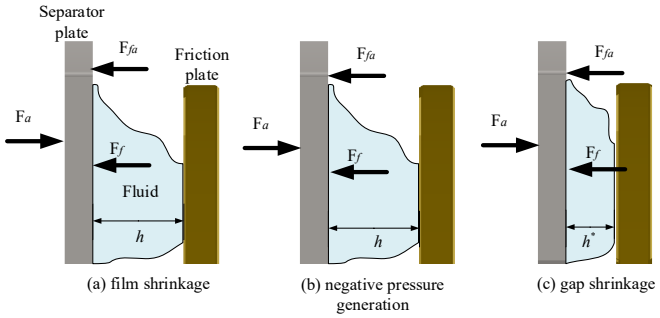

Figure 6: Fluid film change diagram

As shown in Fig 6, when $F_f \geq F_a - F_{fa}$, the film support force is larger than the gas pressure difference between the two sides, and the separator plate will not move. When $F_f < F_a - F_{fa}$, the film support force is smaller than the gas pressure difference, and the separator plate will move close to the friction plate. The gap is reduced until the film support force increases to maintain the equilibrium state. Therefore, the film thickness in each equilibrium state can be obtained by solving Eq. (12):

$$h^* = \sqrt[3]{\frac{6\mu Q\left(-R_s^2 \ln\frac{R_s}{R_o} - R_i^2 \ln\frac{R_o}{R_i} + \frac{R_s^2 - R_i^2}{2}\right)}{\frac{3\pi\rho\omega^2}{40}(R_s^4 - 2R_s^2R_o^2 - R_i^4 + 2R_i^2R_o^2)}} \tag{14}$$

Therefore, the real film thickness is

$$h_o = \begin{cases} h, h^* > h \\ h^*, h^* \leq h \end{cases} \tag{15}$$

The simulation results of h_o are shown in Fig. 7. The film thickness is maintained in low-speed zone and begins to decrease at approximately 1700 rpm.

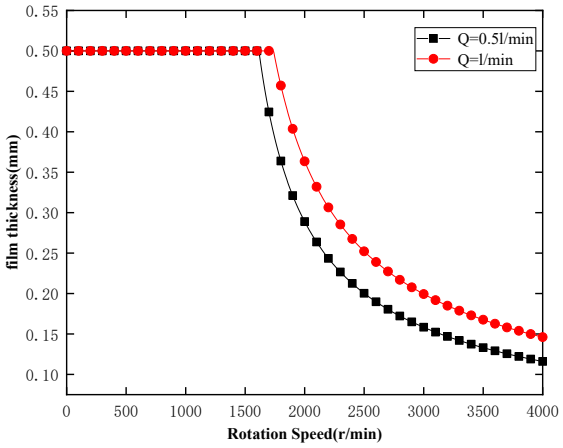

Figure 7: Simulation result of film thickness

The developed DT model can be expressed as

$$T=\int_0^{2\pi}\int_{R_i}^{R_s}\frac{\mu\omega}{h_o}drd\theta \tag{16}$$

3 Experimental system

In this study, the friction element high-speed DT test system was used for verification testing, as shown in Fig. 8. The test bench consists of a main power unit, auxiliary power unit, test box, servo linear actuation system, data acquisition system, and hydraulic system.

The main power unit and auxiliary power unit driven by inverter motor were used to drive the rotation of the friction plate and separator plate, respectively. The main power system is rated at 5,700 rpm, with a maximum speed of 10,000 rpm and rated power of 305 kW. The auxiliary power system is rated at 2,500 rpm, with a maximum speed of 5000 rpm and rated power of 200 kW. A torque sensor was used to measure the speed and torque during the test with a range of ±400/±50 Nm and accuracy of 0.5%.

The test bag was used to install friction plates and separator plates, including inner and outer hubs.

Servo linear actuation system: The servo electric cylinder was used to realize double closed-loop control of friction element pressure and displacement. The maximum pressure of the servo pressure system is 1.7 T, and the displacement control precision is 0.05 mm.

The data acquisition system used the NI data acquisition board to acquire test data from the test bench.

The hydraulic system has the functions of lubrication, cooling, and heating. The flow sensor and proportional valve were used to accurately control the oil flow. The flow can be adjusted from 0.5 to 25 L/min and the control accuracy is 0.1 L/min.

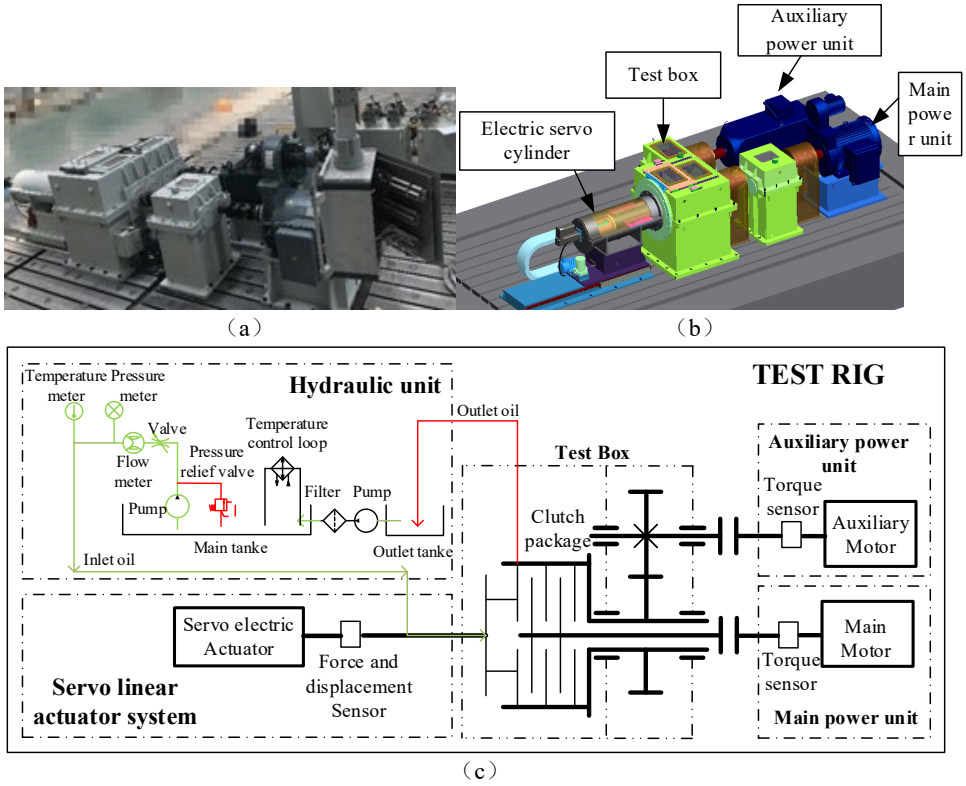

Figure 8: Friction element high-speed DT test system: (a) actual photo of test rig; (b) 3D structure of test rig; and (c) schematic diagram along with hydraulic circuit

During the test, the main power unit drove the friction plate to rotate while the separator plate remained in the braking state. The specific test process is as follows:

a. The lubricating fluid temperature control system is started up to keep the fluid temperature constant.
b. The servo linear actuation system uses force closed-loop control until it detects the sudden change in pressure. Then, saves it as displacement zero and switches to displacement closed-loop control so that the gap reaches the set value.
c. The main power unit drives the friction plate to rotate, and the speed range is 0-4000 r/min. During the speed increase process, constant speed was maintained for 30 s to stabilize the lubricating fluid film. The corresponding torque value at that speed should be recorded to analyze the influence of speed on torque. Considering that the torque in the low-speed zone drastically changed, the recording interval in the low-speed zone is 50 r/min, while the recording interval in the high-speed zone is 200 r/min.
d. Conditions such as flow rate, clearance, friction material, and groove patterns are changed, and the above process is repeated.

The resulting curve of the test conditions listed in Tab. 2 is shown in Fig. 9. In the figure, the torque fluctuates at each moment of change in rotational speed. This torque fluctuation is

caused by the adjustment of the rotational speed of the motor, which can be ignored or smoothed. It can be seen from the curve that there are two turning points in the DT corresponding to the first specific speed and second specific speed. The rotational speeds of the two turning points are called the first critical speed and second critical speed, respectively.

Table 2: Test conditions

Parameters	Values	Parameters	Values
Outer radius *Ro*	m	Flow rate *Qa*	L/min
Inner radius *Ri*	0 m	Gap *h*	0 m
Number of friction pairs	1	Fluid temp	50℃
Material	Copper-based	Groove type	Nongroove

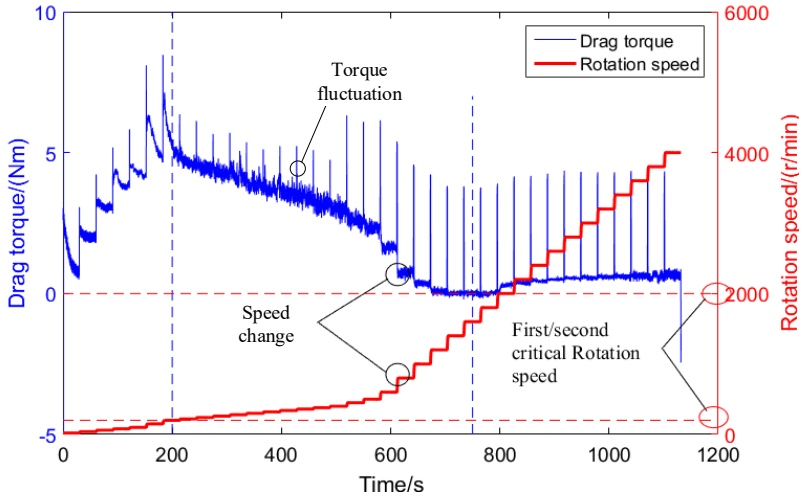

Figure 9: Test results

4 Model validation and discussion

The analysis of the mathematical model showed that the fluid film is no longer continuous when it reaches the first critical speed and is mixed with gas [Wu, Xiao, Hu et al. (2018)]. In order to study the gas distribution, a volume of fluid (VOF) model was established. The inner diameter was set as the speed inlet, which can be calculated according to the flow rate. The outer diameter was set as the pressure outlet, and the value is the standard atmospheric pressure. The two sides of the lubricating fluid film were set as the moving wall and fixed wall, respectively, as shown in Fig. 10.

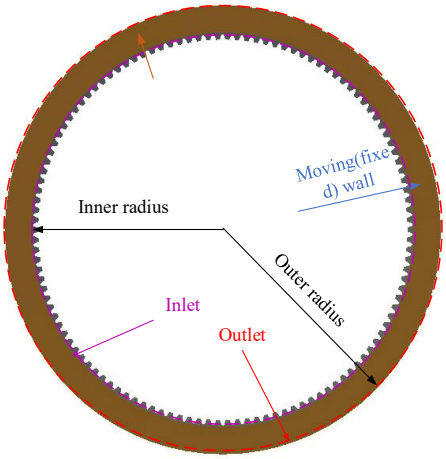

Figure 10: CFD model

The results of the computational fluids dynamics (CFD) simulation model in Fig. 11 show that the gas first appeared near the outer diameter; as the rotational speed increased, the gas continuously penetrated from the outer radial inner diameter direction.

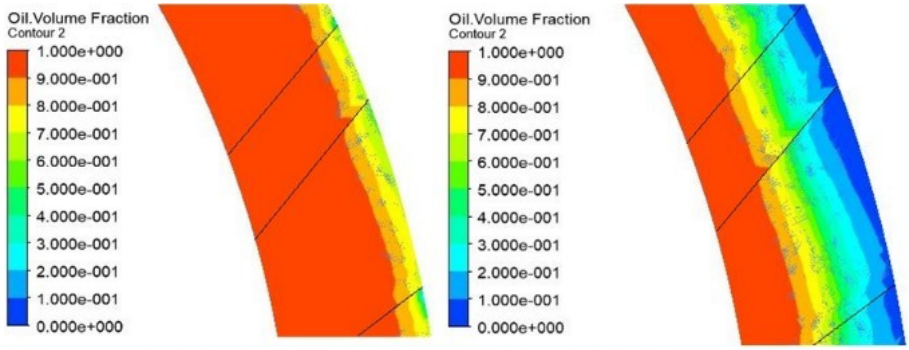

(a) (b)

Figure 11: CFD results: (a) at 400 r/min; (b) at 900 r/min

Fig. 12 is the curve of the fluid phase volume fraction with rotational speed. The mathematical model and CFD model are consistent. The fluid phase volume fraction is 100% at low speed. At this time, the gap is covered by the full fluid film. At high speed, the lubricating fluid film is discontinuous. The fluid phase volume fraction decreases with increasing rotational speed.

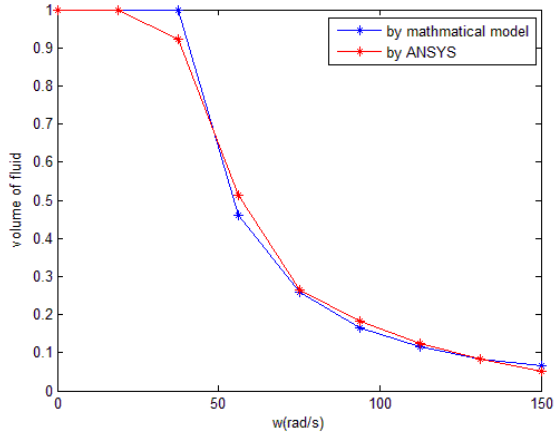

Figure 12: Fluid phase volume fraction

Fig. 13 shows the tendency of the DT with changing rotational speed and the state of the fluid film. The change in DT can be divided into three stages. The first stage: In the state of full continuous fluid film, the DT gradually increases as the speed increases until the first critical speed is reached. The second stage: The fluid film begins to shrink, and the DT gradually decreases as the speed increases until the second critical speed is reached. The third stage: The DT begins to rise as the speed increases. Based on the mathematical model, we found that the fluid film support force decreased to a negative value after the second critical speed, which brought the separator plate and friction plate close to each other to reduce the gap and maintain equilibrium. Pahlovy et al. [Pahlovy, Mahmud, Kubota et al. (2017)] found that the DT of the axial fixed separator plate and friction plate did not not rise at high speed, which confirms the above analysis.

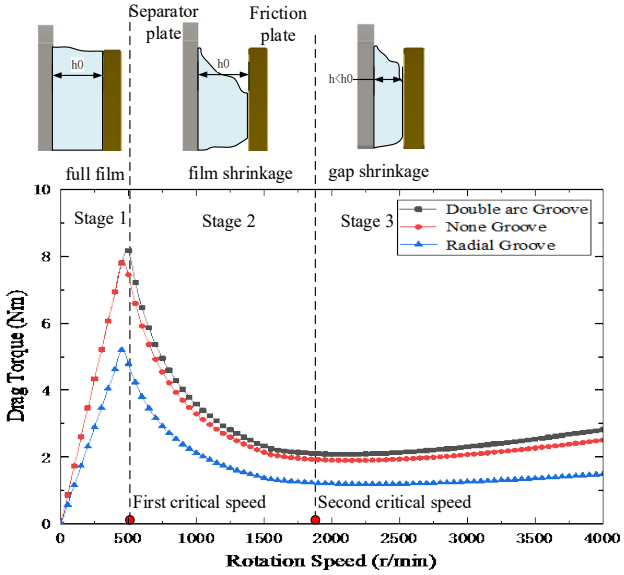

Figure 13: Simulation of three friction plates

It can be seen from Fig. 14 that the test results are consistent with the simulation results on the DT trend. The DT of the nongroove friction plate is the highest, while that of the friction plate with radial grooves is the lowest. The addition of grooves increased the flow required to maintain the full fluid film lubrication, and the equivalent radius decreased, resulting in the decrease in DT. Hence, the DT of the nongroove friction plate is the highest. The DT of the friction plate with radial grooves is lower than that of the friction plate with double arc grooves because the radial grooves occupy a large area, and the flow rate required for full fluid film lubrication is higher.

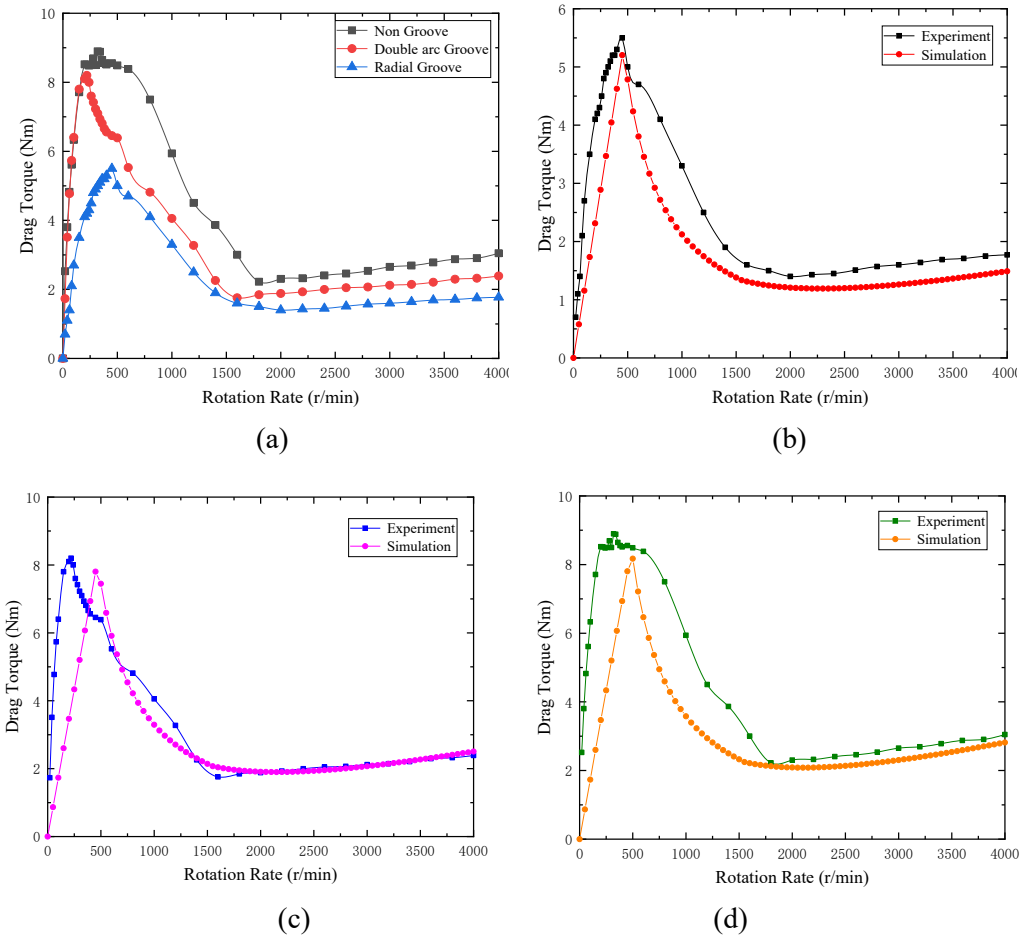

Figure 14: Comparison of test and simulation results: (a) three friction plates; (b) friction plates with radial grooves; (c) friction plates with double arc grooves; (d) nongroove friction plates

4 Conclusions

(a) The tendency of the DT with changing rotational speed can be divided into three stages.

First stage: There exists a full continuous fluid film in the gap, and the fluid is single phase. DT increases with increasing clutch speed.

Second stage: With increased speed, the required flow rate is greater than the supplied flow rate. Thus, the fluid film begins to shrink, and the fluid is two-phase. The DT decreases with increasing speed.

Third stage: As the speed continuously increases, the pressure of the fluid decreases to a negative value, which brings the separator plate and friction plate close to each other, reducing the gap between the plates. The DT increases again with increasing speed.

(b) Based on the VOF model, it is known that at low speed, the gap is full of fluid film. With the increase in rotational speed, the fluid phase volume fraction gradually decreases.

(c) In the case where the other parameters are the same, the DT of the nongroove friction plate is highest, that of double arc grooves is in the middle, and that of radial grooves is the lowest. This is because grooves require more fluid to maintain the full continuous fluid film. The larger the area occupied by grooves, the lower the DT.

Acknowledgement: The authors would like to acknowledge the financial support from the research project of basic product innovation of MIIT (VTDP3203).

References

Aphale, C. R.; Cho, J.; Schultz, W. W.; Ceccio, S. L.; Yoshioka, T. et al. (2006): Modeling and parametric study of torque in open clutch plates. *Journal of Tribology*, vol. 128, no. 2, pp. 341-345.

Hu, J.; Peng, Z.; Wei, C. (2012): Experimental research on drag torque for single-plate wet clutch. *Journal of Tribology*, vol. 134, no. 1, pp. 014502.

Iqbal, S.; Albender, F.; Pluymers, B.; Desmet, W. (2013): Mathematical model and experimental evaluation of drag torque in disengaged wet clutches. *Isrn Tribology*, vol. 2013, no. 12.

Iqbal, S.; Albender, F.; Pluymers, B.; Desmet, W. (2014): Model for predicting drag torque in open multi-disks wet clutches. *Journal of Fluids Engineering*, vol. 136, no. 2, pp. 021103.

Kato, Y. (1993): Fuel economy improvement through tribological analysis of the wet clutches and brakes of an automatic transmission. *Proceedings of JSAE*, pp. 57-60.

Kitabayashi, H.; Li, C. Y.; Hiraki, H. (2003): Analysis of the various factors affecting drag torque in multiple-plate wet clutches. *JSAE/SAE International Spring Fuels and Lubricants Meeting*, pp. 1840-1845.

Li, M.; Khonsari, M. M.; Mccarthy, D. M. C.; Lundin, J. (2014): Parametric analysis for a paper-based wet clutch with groove consideration. *Tribology International*, vol. 802, pp. 22-233.

Lloyd, F. A. (1974): Parameters contributing to power loss in disengaged wet clutches. *SAE Transactions*, vol. 83, pp. 2498-2507.

Mahmud, S. F.; Pahlovy, S.; Kubota, M.; Ogawa, M.; Takakura, N. (2017): A simulation model for predicting high speed torque jump up phenomena of disengaged transmission wet clutch. *SAE Technical Paper*.

Pahlovy, S. A.; Mahmud, S.; Kubota, M.; Ogawa, M.; Takakura, N. (2017): Development of an analytical model for prediction of drag torque characteristics of disengaged wet clutches in high speed region. *SAE Technical Paper*.

Takagi, Y.; Okano, Y.; Miyayaga, M.; Katayama, N. (2012): Numerical and physical experiments on drag torque in a wet clutch. *Tribology Online*, vol. 7, no. 4, pp. 242-248.

Wu, W.; Xiao, B.; Hu, J.; Yuan, S.; Hu, C. (2018): Experimental investigation on the air-liquid two-phase flow inside a grooved rotating-disk system: flow pattern maps. *Applied Thermal Engineering*, vol. 133, pp. 33-38.

Xiang, C.; Zhang, Y.; Liu, H. (2013): Research on drag torque of high relative speed open wet clutch of vehicle. *Journal of Mechanical Engineering*, vol. 49, no. 20, pp. 71.

Yuan, S.; Guo, K.; Hu, J.; Peng, Z. (2010): Study on aeration for disengaged wet clutches using a two-phase flow model. *Journal of Fluids Engineering*, vol. 132, no. 11, pp. 111304.

Yuan, S.; Peng, Z.; Jing, C. (2011): Experimental research and mathematical model of drag torque in single-plate wet clutch. *Chinese Journal of Mechanical Engineering*, vol. 24, no. 1, pp. 91-97.

Yuan, Y; Liu, E. A.; Hill, J. (2007): An improved hydrodynamic model for open wet transmission clutches. *Journal of Fluids Engineering*, vol. 129, no. 3, pp. 333-337.